Max-Planck-Institut für Meteorologie

REPORT No. 77

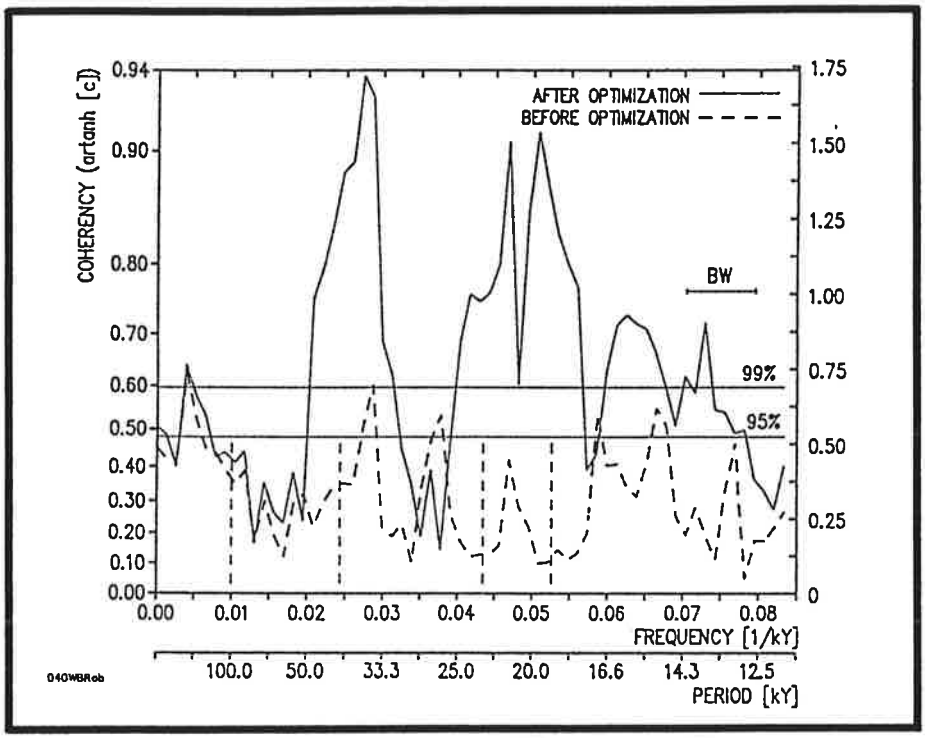

A DIRECT MATHEMATICAL APPROACH TO OPTIMIZE THE AGE-DEPTH RELATION OF DEEP-SEA SEDIMENT CORES

by

WOLFGANG BRÜGGEMANN

HAMBURG, JANUARY 1992

AUTHOR:

WOLFGANG BRÜGGEMANN

MAX-PLANCK-INSTITUT
FÜR METEOROLOGIE

MAX-PLANCK-INSTITUT
FÜR METEOROLOGIE
BUNDESSTRASSE 55
D-2000 HAMBURG 13
F.R. GERMANY

Tel.: +49 (40) 4 11 73-0
Telex: 211092 mpime d
Telemail: MPI.METEOROLOGY
Telefax: +49 (40) 4 11 73-298

ISSN 0937–1060

A Direct Mathematical Approach to Optimize the Age-Depth Relation of Deep-Sea Sediment Cores

Wolfgang Brüggemann

December 20, 1991

Abstract

The question of an optimal age-depth relation for deep-sea sediment cores has been raised frequently. The data from such cores (e.g., $\delta^{18}O$ values) are used to test the astronomical theory of ice-ages as established by Milankovitch in 1938. In this work, we use a direct mathematical approach to find simultaneously an optimal age-depth relation and a linear model that optimally links solar insolation or other model input with global ice-volume. Thus, a general tool for the calibration of deep-sea cores to arbitrary tuning targets is presented. In this inverse modeling type approach, an objective function is minimized that penalizes: 1) the deviation of the data from the theoretical linear model (whose transfer function can be computed analytically for a given age-depth relation) and 2) the violation of a set of plausible assumptions about the model, the data and the obtained correction of a first guess age-depth function. We formulate an unconstrained optimization problem that is solved numerically by conjugate gradient type methods. Using this direct approach, we obtain high coherencies in the Milankovitch frequency bands (over 90%). Not only the data time series, but also the the derived correction to a first guess linear age-depth function (and therefore the sedimentation rate) itself contains significant energy in a broad frequency band around 100 ky. The use of a sedimentation rate which varies continuously on ice-age time

scales results in a shift of energy from 100 ky in the original data spectrum to 41, 23 and 19 ky in the spectrum of the corrected data. However, a large proportion of the data variance remains unexplained, particularly in the 100 ky frequency band, where there is no significant input by orbital forcing. The presented method is applied to a real sediment core and to the SPECMAP stack, and results are compared with those obtained in earlier investigations.

1 Introduction

Proxy data from deep-sea cores have been used extensively to test the orbital theory of ice-ages introduced by Milankovitch [1938]. A problem in the direct comparison between time-dependent forcing (changes in solar insolation) and space- (i.e. depth-) dependent data, however, is that there is no accurate experimental age-dating procedure for the long time intervals considered. Shackleton et al. [1990] suggested that even well–established ages (such as the Brunhes-Matuyama boundary at 730 ky) might be underestimated by up to 7% (780 ky). Recently, this hypothesis has received independent support by Hilgen [1991] using a similar astronomical tuning approach, by Izett and Obradovich [1991] for the case of the Brunhes–Matuyama boundary (new estimate at 790 ky) and by Walter et al. [1991] for later isotopic events from a $^{40}Ar/^{39}Ar$ analysis using a single–crystal laser–fusion technique.

Here, a universal tool for quick testing of orbital and other theories of ice-ages is presented which produces optimal age-depth functions for arbitrary cores, subjective only in terms of the relative importance of the different components of the objective function.

This work pursues two simultaneous goals. First, we try to find an optimal response function for a linear system of arbitrary high order that links solar insolation with climate indices, for example global ice volume as represented by the ratio of stable oxygen isotopes. The solar insolation varies with the geometry of the earth's orbit around the sun, and can be computed numerically for the last million years [Berger, 1978]. In the frequency domain, this input contains

significant energy only in the Milankovitch frequency bands of 41, 23 and 19 ky. In further experiments we use also the sum of the normalized orbital parameters (the so-called ETP time series; cf. Imbrie et al. [1984]) as system input which in addition contains energy in the 100 ky frequency band.

Second, we are looking for an age-depth function for the data such that the difference between model output (as a function of time) and data (as a function of depth in the core) is minimized in the least-squares sense.

In order to achieve these two goals, we formulate an objective function for an unconstrained optimization problem, while making additional requirements for numerical stability and physical plausibility. This idea originally goes back to the work of Hasselmann and Herterich [1983], who suggested minimizing the weighted sum of the following five components:

- the deviation between the model and the data,
- the deviation of the optimal age-depth relation at well-dated points (e.g., the Brunhes-Matuyama boundary) from their ages determined by other means,
- the overall deviation of the optimal age-depth relation from a first guess (which in a standard case is assumed to be a linear interpolation between the present and the Brunhes-Matuyama boundary at 730 ky),
- the square of the second derivative of the new age-depth relation,
- the overall deviation of the optimal linear model from a preferred linear model (which in the following is assumed to be of first order).

Hasselmann and Herterich suggested that this optimization problem could be solved by an iterative process of integrating Euler's equations and computing the transfer function of the optimal linear model analytically. In this paper we begin with a similar weighted objective function that includes an additional term to assure a monotonically increasing age-depth relation. However, this objective function is subsequently minimized directly by a conjugate-gradient type algorithm where derivatives are computed numerically.

The procedure for determining an optimal age-depth relation of deep-sea cores is tested by applying it to data of the Meteor core M 13519 [Sarnthein et al., 1984] and to the SPECMAP stack [Imbrie et al., 1984]. The results are compared with earlier studies by Herterich and Sarnthein [1984], Shackleton and Matthews [1977], Imbrie et al. [1984] and Herterich [1988].

A rather similar approach has recently been explored by Grieger [1991]. In his work a function $t(z)$ is introduced that maps points in the core to the corresponding ages; this is the reverse of the $z(t)$ mapping adopted here. Grieger's objective function and the model restrictions are formulated in the time domain rather than the frequency domain.

The most widely applied method for dating cores for the last 900 ky is the approach used by Imbrie et al. [1984] to establish the SPECMAP age-depth relation. Following the initial work by Hays et al. [1976] the SPECMAP age-depth relation was obtained by passing the orbital parameters (obliquity and precession index) rather than the solar insolation through an exponentially damped system with a time constant of 17 ky. The output curve obtained (ETP) was used as the target for the filtered data curves. The best fit was determined iteratively for the different frequency bands by phase locking the data to the orbital parameter curves and averaging over several cores.

Martinson et al. [1987] give a high-resolution chronostratigraphy for the last 300 ky by averaging the results of four different orbital tuning approaches. Each of these approaches was based on different assumptions:

- The "Phase Locked Approach" assumes constant phase between dominant components of orbital forcing and the corresponding components in the geological data.
- The "Direct Response Approach," where the response is assumed to mimic the forcing, consistent with the original Milankovitch theory.
- The "Nonlinear Response Approach" uses the non-linear model of Imbrie and Imbrie [1980] consisting of two simple linear models with different time constants for warming and cooling.

- The "Pure Components Approach" is comparable to the original idea of Hays et al. [1976], further developed by Imbrie et al. [1984] as mentioned above. Here the tuning target is constructed from the linear combination of "pure" (i.e. orbital rather than solar insolation) components and their harmonics.

The final chronology was determined to have an average error of 5 ky. This error analysis is based on averaging over different tuning approaches which are all assumed to be equally plausible.

Shackleton and Matthews [1977] derived a depth-time relation by directly correlating coral terraces in Barbados with the oxygen isotope stratigraphic record. Herterich and Sarnthein [1984] tested three different approaches using data from Meteor core M 13519. They obtained the initial age-depth function "LIN" by linear interpolation between radiometrically dated points. The "CARPOR" age-depth relation is also based on radiometric data and was developed under the twin assumptions of constant accumulation rate of aeolian dust near the thermal equator and the influence of differential porosity and calcium-carbonate dissolution on the short-term sedimentation rates. Two further age-depth relations were again obtained by orbital tuning ("TUNE" and "STUNE"). The second approach differs from the first by keeping the isotopic stage boundary 5/6 (cf. Sarnthein et al. [1984] and Prell et al. [1986]) and the Brunhes-Matuyama magnetic reversal fixed at 127 ky and 730 ky, respectively. The goal of both approaches was to maximize squared coherency, which reaches values of up to 75%.

Herterich [1988] considers an objective function similar to that originally developed by Hasselmann and Herterich [1983]. The optimal model (of arbitrary high order) and the preferred model are assumed to be identical, and an age-depth relation is found for the last 300 ky. The solution is again obtained by an iterative process of integrating Euler's equation for the age-depth function and optimizing the objective function with respect to the remaining model parameters.

Recently, Shackleton et al. [1990] suggested that over the last 2000 ky a better match with orbital models could be obtained with a timescale departing from

the established SPECMAP timescale below 620 ky (isotopic stage 16 as defined by Shackleton and Opdyke [1973]. As a consequence the Brunhes-Matuyama boundary was dated at 780 ky instead of 730 ky.

2 A Simple Model

In this work, two different models are used to relate the $\delta^{18}O$ data (that are assumed to represent global ice-volume) and the assumed solar forcing $r(t)$ or $R(f)$. (In the following, time series are denoted by lower case letters in the time domain and upper case letters in the frequency domain. All time series are furthermore assumed to be normalized to zero mean and unit standard deviation.) In the first case an arbitrary linear model is introduced that can be described by its impulse or frequency response functions h and H, respectively. The output of this system, the theoretical global ice volume, y or Y, is represented by the convolution of the impulse response function and the input r

$$y(t) = \int_{-\infty}^{\infty} h(t-u)r(u)du, \tag{1}$$

or equivalently by the product of frequency response function and input representation in the frequency domain

$$Y(f) = H(f)\ R(f). \tag{2}$$

In the second case we consider a preferred model with response functions h_0 or H_0 that is typically of low order and can be specified by a stochastic differential equation. For the following we assume for simplicity and consistency with Hasselmann and Herterich [1983] and Herterich [1988], that the output, y_0 or Y_0, of this preferred system is given by

$$\frac{d}{dt}y_0(t) = -\lambda y_0(t) + \alpha r(t), \tag{3}$$

although linear systems of higher order are also permissible and can be easily implemented in the numerical method used. Here α and λ are parameters of the preferred model that can also be used for improving the fit. The frequency response function of the preferred system (3) is given by

$$H_0(f) = \frac{\alpha}{2\pi i f + \lambda}. \tag{4}$$

The variance of the output time series of these two models, y and y_0, will be compared with the variance of the core data.

3 Data

Deep-sea cores contain information on the ratio of heavy ^{18}O and normal ^{16}O oxygen isotopes. This ratio is believed to be strongly correlated to the global ice volume and is used as an indicator for ice-ages [Imbrie et al., 1984]. The data obtained from deep-sea cores are given as a function of depth in the core by

$$\delta^{18}O(c) := \frac{f_{18,16}(c) - \hat{f}_{18,16}}{\hat{f}_{18,16}}. \tag{5}$$

Here $f_{18,16}(c)$ stands for the ratio between heavy ^{18}O isotopes and normal ^{16}O isotopes at depth c and the reference value $\hat{f}_{18,16}$ denotes the isotopic ratio of sea water for 1950. Linear interpolation is used to complete the $\delta^{18}O$ curve (5) between actually sampled points in the core. In figure 1 the normalized $\delta^{18}O$ values of the core M 13519 from the Sierra Leone Rise ($5°39,5'N, 19°51'W$) are plotted versus depth [Sarnthein et al., 1984].

To test theories of ice-ages, the isotopic data must be converted from depth to time dependent data. Starting from an initial first guess age-depth relation c_0 we introduce a correction x to obtain a new age-depth function

$$c_{new}(t) = c_0(t) + x(t). \tag{6}$$

The data curve then becomes a function of time and the age-depth correction x

$$y_{dat}(x,t) = \delta^{18}O(c_{new}(t)) = \delta^{18}O(c_0(t) + x(t)). \tag{7}$$

In the following, the physical length of the core is denoted by l and this point is assumed to be well-dated at time τ. The value $t = 0$ corresponds to the present condition. The first guess age-depth relation c_0 and the correction term x are assumed to satisfy

$$c_0(0) = 0 \approx x(0)$$

and

$$c_{new}(-\tau) = c_0(-\tau) + x(-\tau) \approx l.$$

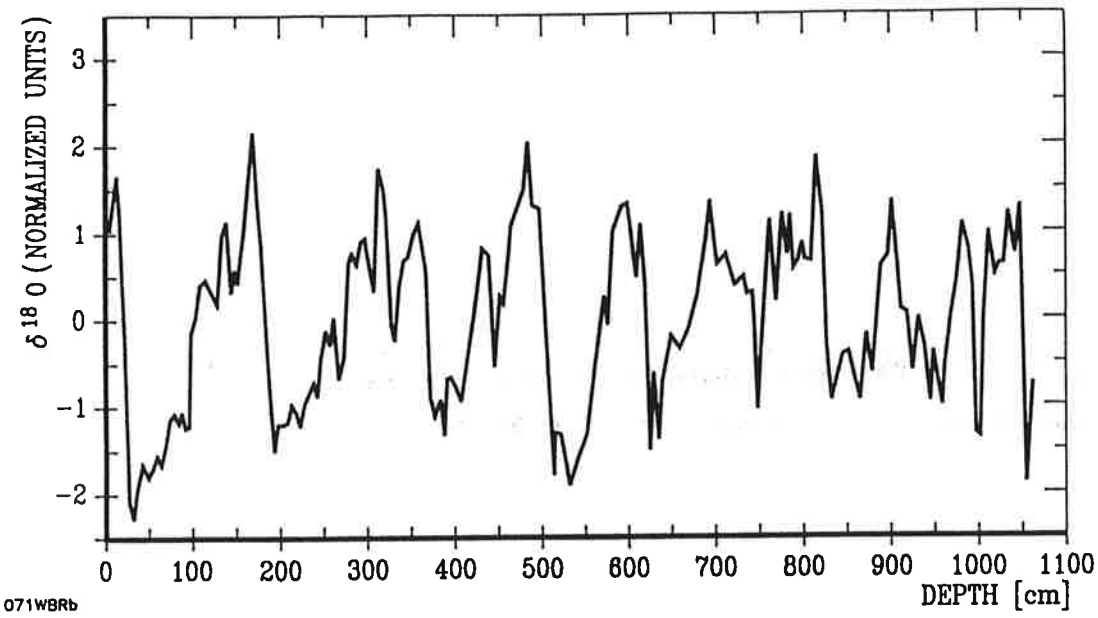

Figure 1: δ^{18}O data curve of Meteor core M 13519 (from Sarnthein et al. [1984])

It should be noted here that y_{dat} is subject to different types of error. These include sampling errors within the core (i.e., errors associated with the selected sampling interval), disturbances due to the process of coring and in situ disturbances at the ocean floor (e.g., bioturbulence and changes in currents). Thus y_{dat} is only one realization of the theoretically infinite ensemble of realizations of the stochastic process underlying the data. The fitting of the data y_{dat} to the model output is done in the spectral domain. Averaging over neighboring frequencies (or, equivalently, over chunks using corresponding time windows) is used to obtain consistent estimators of the power and cross spectra. In the following, averaging is performed using a rectangular window in the frequency domain with moving averages always computed over 7 frequencies (14 degrees of freedom). This averaging process is denoted by cornered parentheses $< \cdot >$.

In the standard case the variation of the solar insolation at 65°N at July 15th is used as system input, since the solar insolation during the summer at high northern latitudes is believed to be crucial for ice build up (cf. Milankovitch [1938] or more recently Crowley and North [1991]). The numerical computation of the solar insolation at a given time uses the method of Berger [1978].

4 Objective Function

In this section we establish the objective function for the global, unconstrained minimization problem following the original idea by Hasselmann and Herterich [1983]. The objective function F consists of the weighted sum

$$F = \sum_{i=1}^{6} g_i F_i$$

of six terms F_1 to F_6. The numbers g_1 to g_6 serve two purposes: First, they reflect the individual preference regarding the relative importance of the different components. Second, they are used to normalize the different components for numerical stability of the optimization procedure. The sensitivity of the optimization problem to changes in the weights is discussed later.

The first term represents the mean square difference between model output y and data y_{dat},

$$F_1 = \int_{-\tau}^{0} < (y(t) - y_{dat}(x,t))^2 > dt \tag{8}$$

or by Parseval's theorem equivalently in the frequency domain

$$\begin{aligned} F_1 &= \sum_{j=-\infty}^{\infty} < |Y(f_j) - Y_{dat}(x,f_j)|^2 > \\ &= \sum_{j=-\infty}^{\infty} < |H(f_j)R(f_j) - Y_{dat}(x,f_j)|^2 > . \end{aligned} \tag{9}$$

The averaging over neighboring frequencies or the equivalent local averaging process in the time domain indicated by $< \cdot >$ (as an estimationn of a hypothetical statistical ensemble average) is redundant here but is introduced as it will be required later for cross spectrum estimation in computing the transfer function H of an optimally-fitted linear system. It should be pointed out here that the Fourier transform of the data time series Y_{dat} depends also on the correction x of the first guess age-depth function.

Second, the corrected age-depth function should not deviate too strongly from the first guess c_0 (see equation (6)). This requirement is expressed by the next component

$$F_2 = \int_{-\tau}^{0} x(t)^2 dt. \tag{10}$$

Furthermore, the correction function should be as smooth as possible and should, in particular, it should not contain sharp peaks which would permit the "swallowing" of complete cycles of the data at times where there is little energy in the data. Therefore the third penalty term is

$$F_3 = \int_{-\tau}^{0} \left(\frac{d^2 x(t)}{dt^2} \right)^2 dt. \tag{11}$$

As mentioned above, certain layers in the core may already be well-dated by other (possibly radiometric) methods (e.g., Brunhes-Matuyama boundary). Such well-dated points should not be changed substantially in the optimized age-depth function. Thus, a fourth penalty component

$$F_4 = \sum_{k=1}^{K} (c_k - c_{new}(t_k))^2 \tag{12}$$

is introduced, where c_k, t_k $(k = 1, \ldots, K)$ denote the depths and times, respectively, of well dated points.

The optimal linear model should be consistent with and provide some information about a plausible physical model. Thus, we require through the fifth penalty term that the model should be close to the preferred model or model class characterized by a finite number of parameters (see equation (3) with two parameters α and λ),

$$F_5 = \sum_{j=-\infty}^{\infty} < |R(f_j)|^2 > |H(f_j) - H_0(f_j)|^2. \tag{13}$$

The first five components of the objective function are essentially the same as suggested by Hasselmann and Herterich [1983]. For practical purposes (especially if the weight g_1 is chosen too large) it is necessary to include a sixth condition that prevents the age-depth relation from reversing in time. Thus a very large penalty is introduced for age-depth functions which do not increase monotonically:

$$F_6 = \int_{-\tau}^{0} \left(\chi(t) \, \frac{d}{dt} c_{new}(t) \right)^2 dt, \tag{14}$$

where

$$\chi(t) = \begin{cases} 1 & \text{if } \frac{d}{dt} c_{new}(t) \leq 0 \\ 0 & \text{otherwise.} \end{cases}$$

In addition to these requirements one could specify a preferred value or range for the parameters of the preferred model. For example, negative α and λ in the model (3) are physically meaningless. Again, such constraints can be formulated as least-squares terms and added to the objective function with appropriate weights.

In summary, we construct an objective function

$$F(x, H, \alpha, \lambda) = \sum_{i=1}^{6} g_i F_i(x, H, \alpha, \lambda), \tag{15}$$

that depends on the age-depth correction x, the optimal transfer function H and the parameters of the preferred system (which we will take in the following to be α and λ in accordance with the first-order preferred model given in (3)). For given values of the correction $x(t)$ and the parameters α and λ, the optimal transfer function can be computed analytically at every frequency (since we consider only a finite interval of data, the variables in the frequency domain are discrete with $\Delta f = 1/\tau$). From the minimal condition

$$\begin{aligned}
0 &= \frac{\partial F}{\partial H(f_j)} \\
&= 2g_1 < \overline{R(f_j)}(H(f_j)R(f_j) - Y_{dat}(x, f_j)) > \\
&+ 2g_5 < |R(f_j)|^2 > (H(f_j) - H_0(f_j)) \\
&= 2H(f_j)\,(g_1 + g_5) < |R(f_j)|^2 > \\
&- 2g_1 < \overline{R(f_j)}Y_{dat}(x, f_j) > \\
&- 2g_5 < |R(f_j)|^2 > H_0(f_j)
\end{aligned}$$

we obtain

$$H(f_j) = \frac{g_1 < \overline{R(f_j)}Y_{dat}(x, f_j) > + g_5 H_0(f_j) < |R(f_j)|^2 >}{< |R(f_j)|^2 > (g_1 + g_5)}, \tag{16}$$

where the overbar denotes complex conjugates.

For $g_5 = 0$ one recovers the standard optimal linear model solution. In the case that both parameters g_1 and g_5 are positive, the numerator in equation (16) induces a shift from the estimator of the cross spectrum $< \overline{R(f_j)}Y_{dat}(x, f_j) >$ towards the transfer function of the preferred system $H_0(f_j)$. Substitution of the optimal transfer function (16) into the objective function (15) yields then a simpler cost function

$$F(x, \alpha, \lambda) = \sum_{i=1}^{6} g_i F_i(x, \alpha, \lambda), \tag{17}$$

that depends only on the correction $x(t)$ and the parameters α and λ.

Discrete Objective Function

For numerical implementation the objective function F must be discretized. We assume a uniform discretization $t_i = -\tau + i\Delta t$ $(i = 1, \ldots, M)$ in the time interval $I = [-\tau, 0]$. The continuous correction $x(t)$ is then replaced by a vector $x = (x_1, \ldots, x_M)^T; x_i = x(t_i)$. For the formal minimization algorithm, the parameters of the preferred model are added to the independent vector x, forming the last two components x_{M+1} and x_{M+2}. For a given vector $x := (x_1, \ldots, x_{M+2})^T$, the frequency response $H_j := H(f_j)$ of the optimally fit linear system is computed from (16) at all M frequencies f_j. H_j depends not only on frequency but also on the correction and parameter vector x, $H_j =: H_j(x)$. At all time nodes it is now possible to compute the output of the optimally fitted linear system $y(t_j)$ as the discrete inverse Fourier transform of $Y = HR$. Again, this output depends on the independent vector x, $y_j(x) := y(t_j)$. The transfer function of the preferred linear system depends also on x

$$H_{0,j}(x) := H_0(f_j),$$

since the last two components of x are the parameters α and λ. The discretized objective function is thus given by

$$\begin{aligned} F(x) &= g_1 \sum_{j=1}^{M} (y_j(x) - y_{dat}(x_j + c_0(t_j)))^2 \\ &+ g_2 \sum_{j=1}^{M} x_j^2 \\ &+ g_3 \sum_{j=2}^{M-1} \left(\frac{x_{j-1} - 2x_j + x_{j+1}}{\Delta t^2} \right)^2 \\ &+ g_4 \sum_{k=1}^{K} (c_k - (c_0(t_{j(k)}) + x_{j(k)}))^2 \\ &+ g_5 \sum_{j=-M/2+1}^{M/2} < |R(f_j)|^2 > |H_j(x) - H_{0,j}(x)|^2 \\ &+ g_6 \sum_{j=1}^{M-1} \chi_j^2 (c_{new}(t_{j+1}) - c_{new}(t_j))^2, \end{aligned} \tag{18}$$

where

$$\chi_j = \begin{cases} 1 & \text{if } c_{new}(t_{j+1}) - c_{new}(t_j) \leq 0 \\ 0 & \text{otherwise.} \end{cases}$$

This defines a discrete, non-linear, least-squares optimization problem with an objective function that maps the $M+2$-dimensional Euclidean space to the real line.

The non-linear dependence of the optimization problem should not be confused with the most probably non-linear relation of solar insolation and global ice volume, although the dynamical models used to describe this relation are linear. The optimization problem is non-linear, since the independent vector x basically consists of the individual components of the age-depth function and its input to the objective function is given by the value of the interpolated data function at that time. One particular problem is that the objective function is not differentiable due to the linear interpolation used in between the points where the data were sampled in the core originally. This problem can be overcome, however, by cubic spline interpolation. A comprehensive discussion of optimization algorithms such as Gauss-Newton or Quasi-Newton methods, as well as the treatment of numerical problems such as stability, convergence of algorithms and preconditioning can be found in Gill et al., [1981]. The numerical difficulties of this particular problem are discussed in detail in Brüggemann [1990].

5 Numerical Results

The discrete objective function F in equation (18) is a non-linear least-squares function with non-continuous first derivatives. In the following we shall consider some typical applications with $M+2=130$ variables, where the vector x contains 128 ($\Delta t = 6$ ky) time node components (this allows a straight forward application of standard FFT-algorithms) and two components representing the parameters α and λ of the preferred model. Least-squares problems with many degrees of freedom are usually poorly conditioned. The discontinuities of the first derivative further reduce the stability. We therefore applied a rather robust and fast optimization algorithm called PLMA (Preconditioned Limited Memory Quasi-Newton Algorithm, cf. Gill and Murray [1979]).

Numerical approximations of the first derivatives were used. Initially, forward differences were used until these approximations failed a simple test (computing

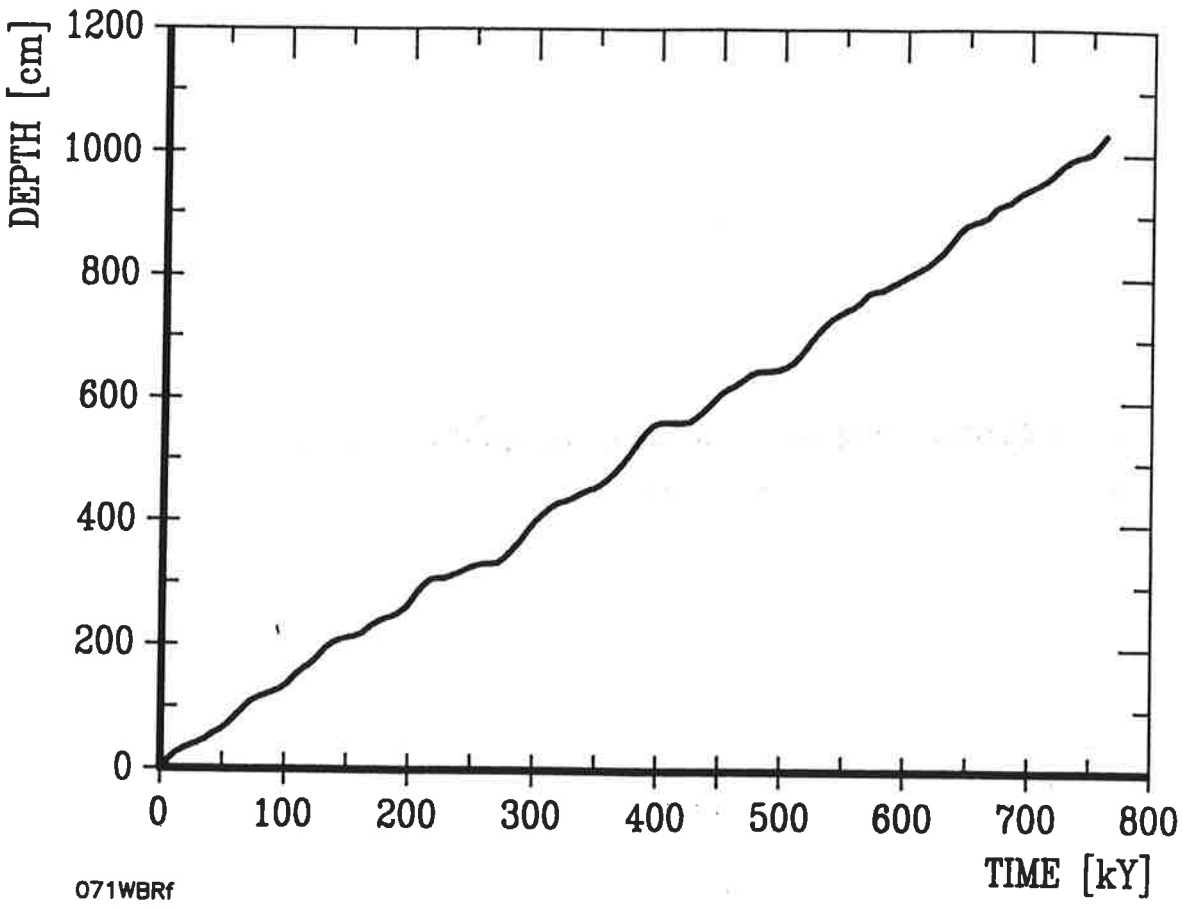

Figure 2: The standard run optimal age-depth function for Meteor core M 13519.

directional derivatives either directly or as a scalar product of the gradient and the chosen unit direction). This usually occurs in the vicinity of an optimum, and we then switched to the more time consuming central differences for higher accuracy.

Standard Case

As a standard case we consider the $\delta^{18}O$ data from the Meteor core M 13519 (figure 1) [Sarnthein et al., 1984]. Starting from a linear interpolation between the present and the Brunhes-Matuyama boundary at 730 ky as the first guess age-depth function, the optimization procedure produces a correction that shifts certain time nodes up to 24 ky (32 cm) in the core. In the following, the resulting age-depth function shown in figure 2 is referred to as the standard run. The net correction (figure 3) has large variations with typical cycle lengths in a broad frequency band at approximately 100 ky (more precisely with peaks at 80 ky and 250 ky).

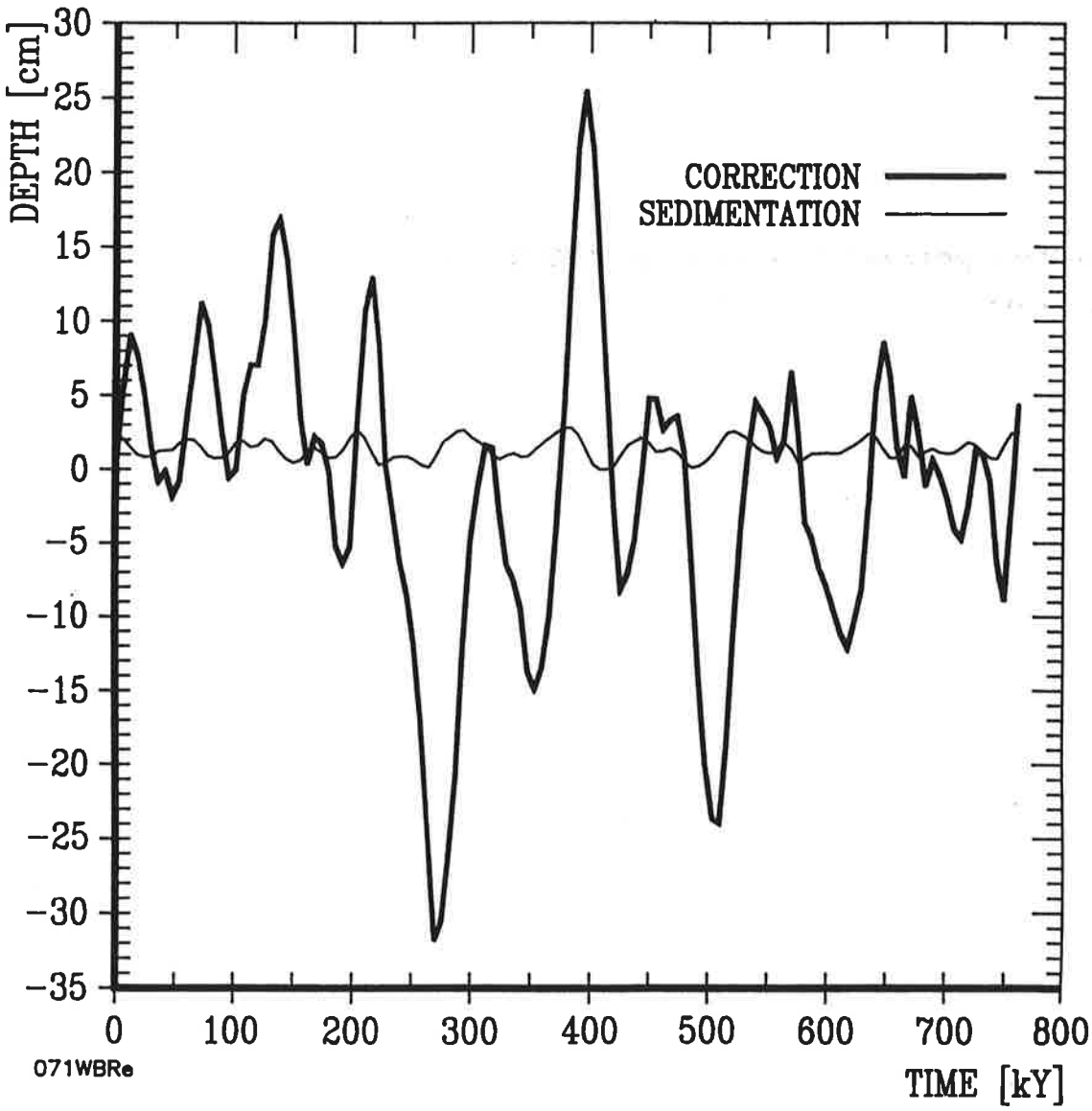

Figure 3: The optimal correction x to the first guess age-depth function (bold line). The thin line shows the sedimentation rate for the standard run.

For this age-depth relation, coherency values between data and solar insolation are obtained that exceed the 99% confidence limits in all three Milankovitch frequency bands 19, 23 and 41 ky (cf. top panel in figure 4). It is important to note that the coherencies obtained are dependent upon the averaging procedure used. In this work we used a relatively wide, rectangular window (14 real degrees of freedom) in the frequency domain. In general, the confidence levels at a given frequency for stochastic estimators associated with a certain averaging technique depend not only on the number of degrees of freedom used for averaging, but also on the bandwidth of the spectra at that frequency. In this case the bandwidth of solar insolation at, for example, 41 ky is not as wide as the window used in the frequency domain. Thus the confidence limits for coherency depend in our case on frequency. For simplicity and comparability with other investigations [e.g., Imbrie et al., 1984] the standard confidence limits in accordance with Jenkins and Watts [1968] have been given in figure 4.

The phase shifts of the data relative to the solar insolation (top panel in figure 5) are negative in the Milankovitch frequencies. This is a necessary condition for our linear model to be causal (it implies that the physical quantity represented by the data follows the solar insolation). On the other hand, the phase shifts at 41 and 23 ky are larger than the shift at 19 ky, which implies instability in the case of a first order model (for models of arbitrary high order, as for example H, this does not violate any stability condition). However, the 95% confidence limits for the phase shifts, which depend on the associated coherency [Jenkins and Watts, 1968], extend to the phase shift curve of the preferred model, which is given by

$$\psi(f) = \arctan(\frac{-2\pi f}{\lambda}). \tag{19}$$

It should be pointed out that neither the coherency nor the phase agreement with the preferred model was maximized here, in contrast to other investigations. For this particular problem these two goals are almost contradictory. To maximize the coherency between data and solar insolation, the weight g_5 in (18) should be small compared to g_1. The transfer function (16) will then be dominated by the cross spectrum of input and data and the coherency will approach the maximal possible value for an arbitrary linear model. If, on the other hand, the weight g_5 is chosen relatively large compared to the other weights, the optimal transfer function will be dominated by the frequency response function of the preferred

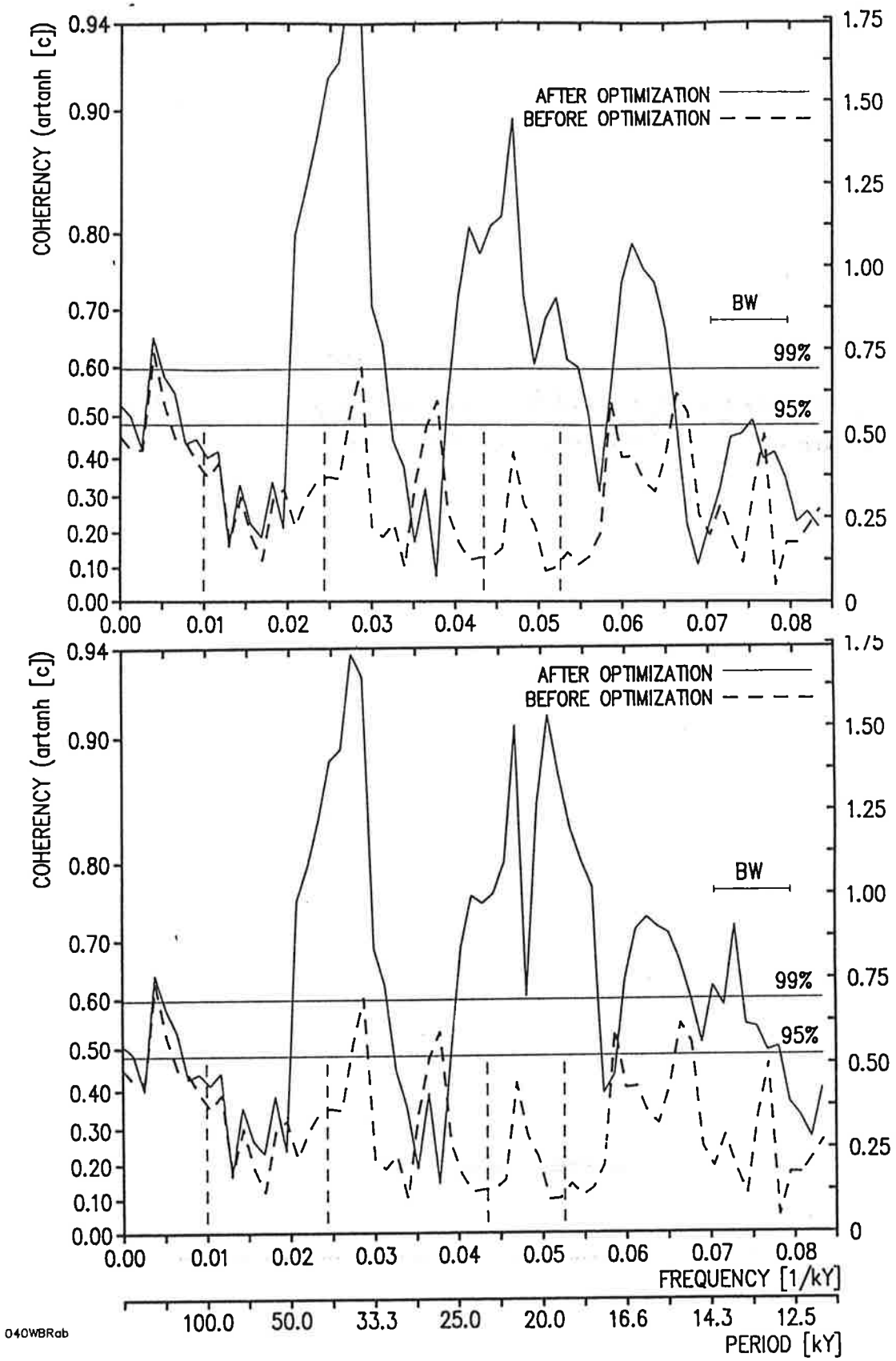

Figure 4: Coherency between system input (solar insolation) and $\delta^{18}O$ before (dashed line) and after (solid line) optimization with side constraints $\lambda > 0$ (top panel) and without side constraints (bottom). Horizontal lines indicate the 95% and 99% confidence limits on an artanh scale (cf. Jenkins and Watts [1968] and page 16).

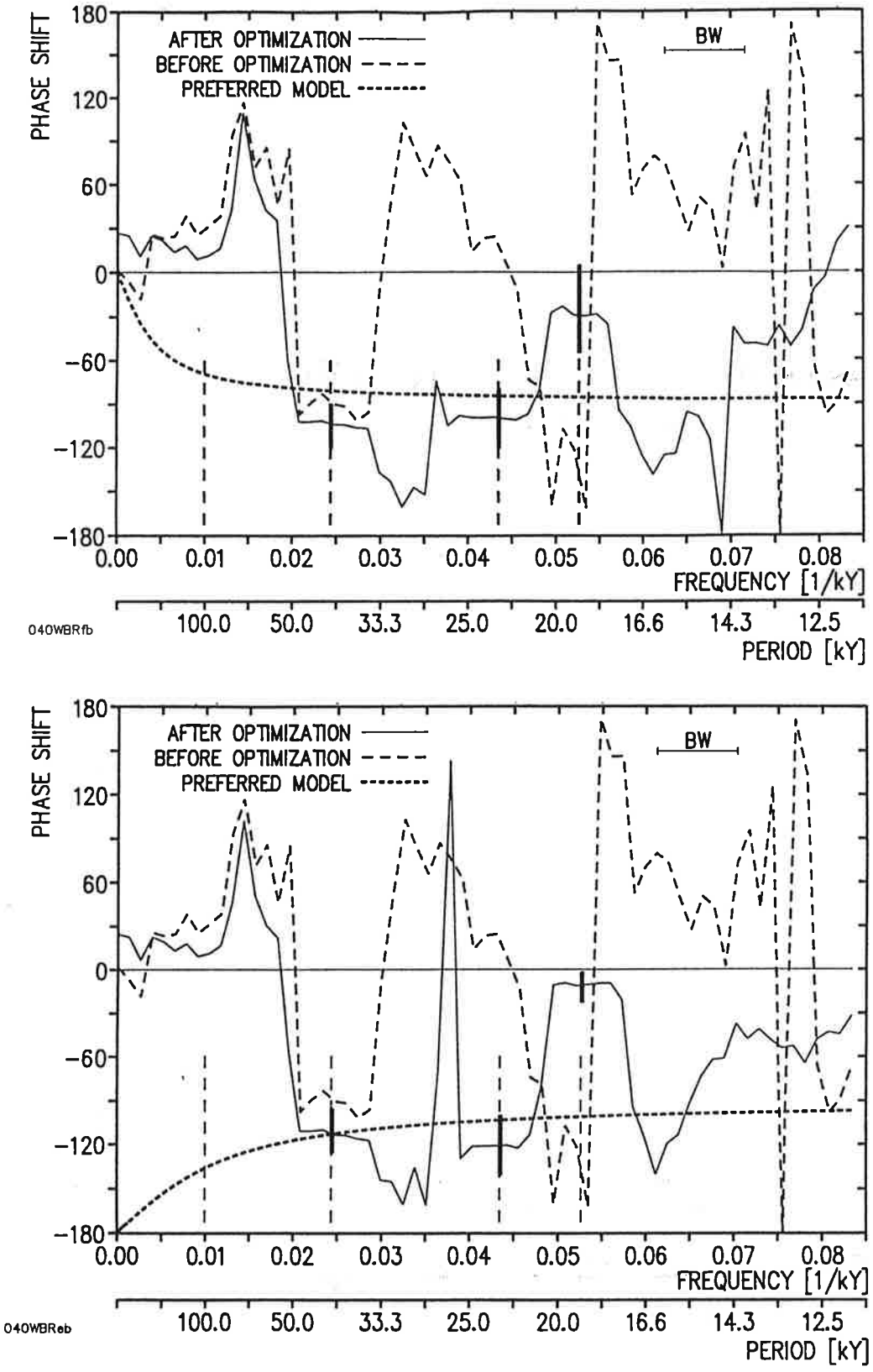

Figure 5: Phase shifts of the data against system input before (dashed lines) and after (solid lines) optimization procedure (solid line) with side constraints $\lambda > 0$ (top panel) and without side constraints (bottom). The dotted line shows the preferred model.

model, and the agreement in phase with the preferred model will be good, at the expense of the coherency (cf. Herterich [1988]).

The amplitudes of the transfer functions are plotted in figure 6, while the data spectra before and after optimization are shown in figure 7. By using a sedimentation rate which varies on the same time scale as the ice-ages, a transfer of energy can be observed from the 100 ky cycle band of the data spectrum before optimization into the 41, 23 and 19 ky frequency bands of the spectrum after the optimization process. The sedimentation rate varies between approximately 0 and 3 cm/ky. A comparison of the different data and model time series is shown in figure 8.

For a physically plausible interpretation of the preferred model the parameters α and λ must be positive. Positive λ is required for stability of the preferred system, while positive α implies smaller ice sheets for larger insolation. Yet, the mathematical problem of minimizing objective function F in (18) is well posed even for arbitrary α and λ. Higher coherencies between data and system input are obviously obtained in a solution in which λ is allowed to become less than zero. The fifth component of the objective function (13) then no longer represents the distance between the frequency response function H and the transfer function of a physical preferred system, but gives instead an approximation target for H in form of a complex function of frequency that depends in addition on two parameters. The actual position in the complex plane of the optimal transfer function in the Milankovitch frequencies does not depend strongly on the sign of λ (figure 9). Experiments (figure 4 and 5) show that the influence of the sign (i.e., the shape of the complex approximation target) on the resulting age-depth relation and the obtained coherencies and phase shifts is rather small. However, if α is sign-constrained and $1/\lambda$ is assumed to lie in the interval between 10 ky and 100 ky, then the optimal time constant obtained is 41.7 ky, while the optimal value for $1/\lambda$ without further constraints is -15.2 ky.

The data spectrum before optimization contains significant energy only in the 100 ky frequency band (figure 7, top panel). After the age-depth function has been optimally adjusted, the data spectrum also contains energy in the Milankovitch frequencies (cf. figure 7, bottom panel). However, a large part of the

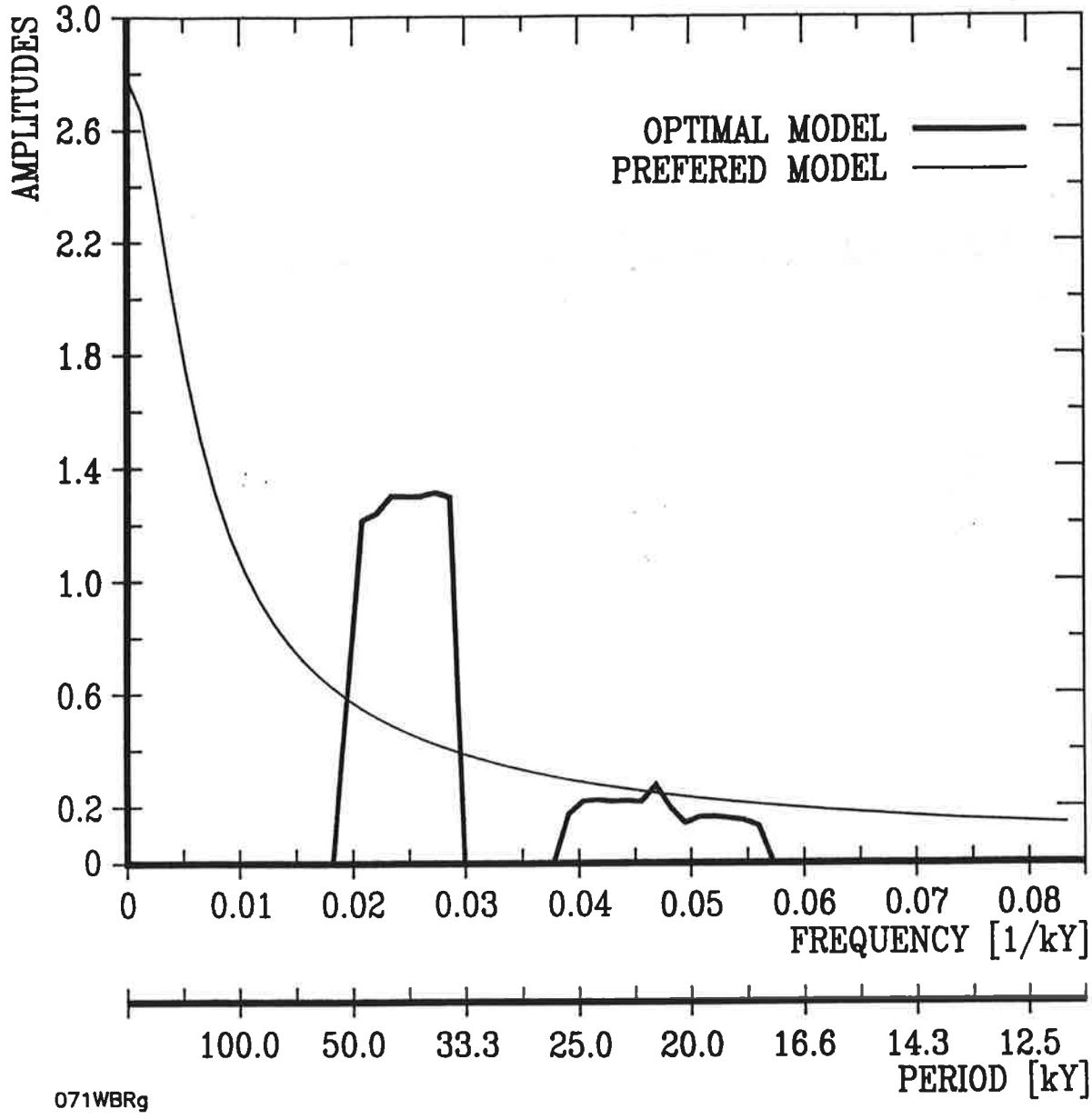

Figure 6: Optimal transfer function (bold line) plotted only where the system input contains significant energy and the transfer function of the preferred model given by equation (4) (thin line).

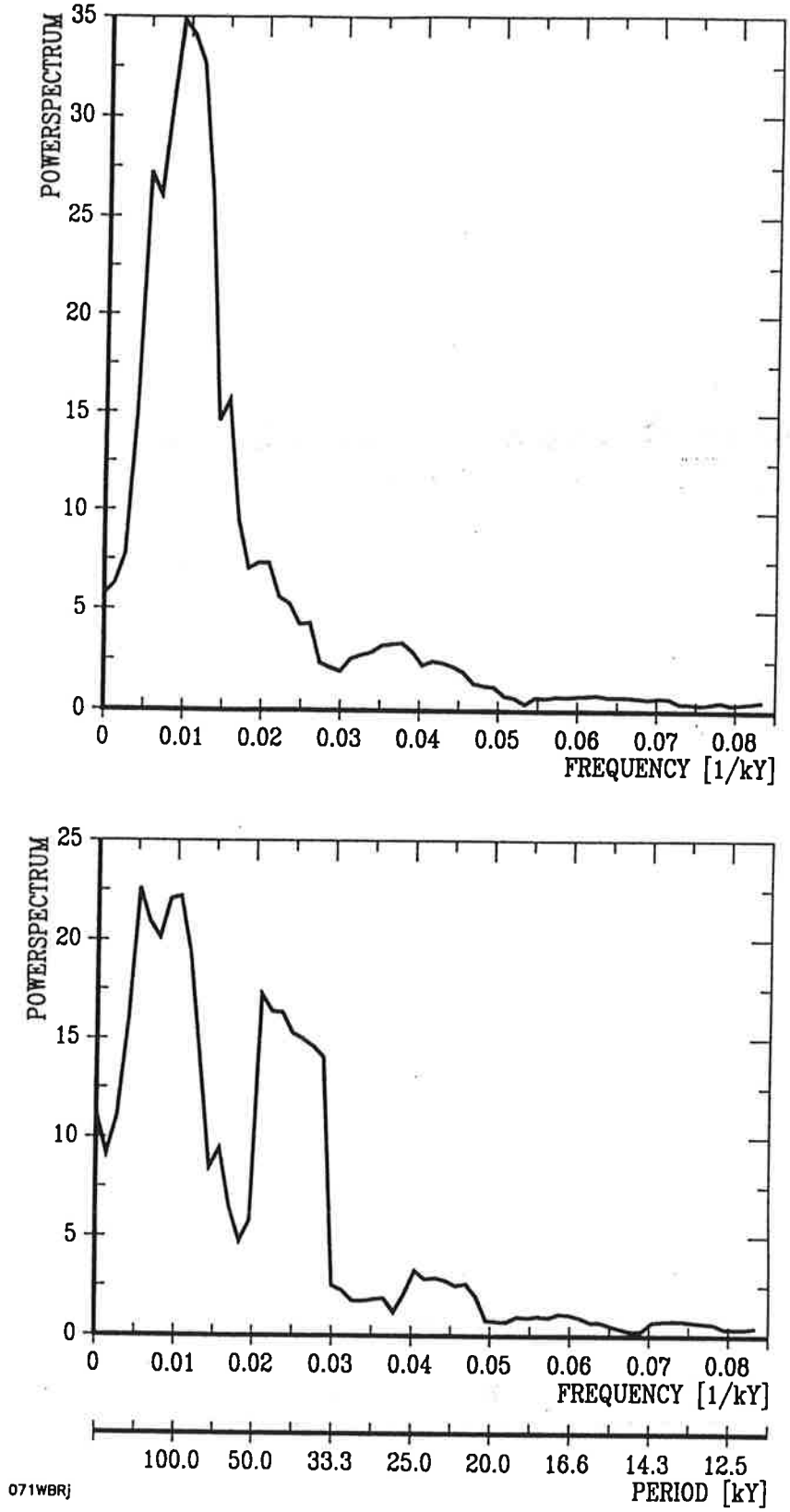

Figure 7: Power spectra estimates for the $\delta^{18}O$ time series before (top) and after (bottom) optimization. It should be noted that for clarity the spectral estimates are plotted here on a linear scale in contrast to the power spectra shown in figure 10 till figure 15, which were plotted on a logarithmic scale as suggested by Jenkins and Watts [1968].

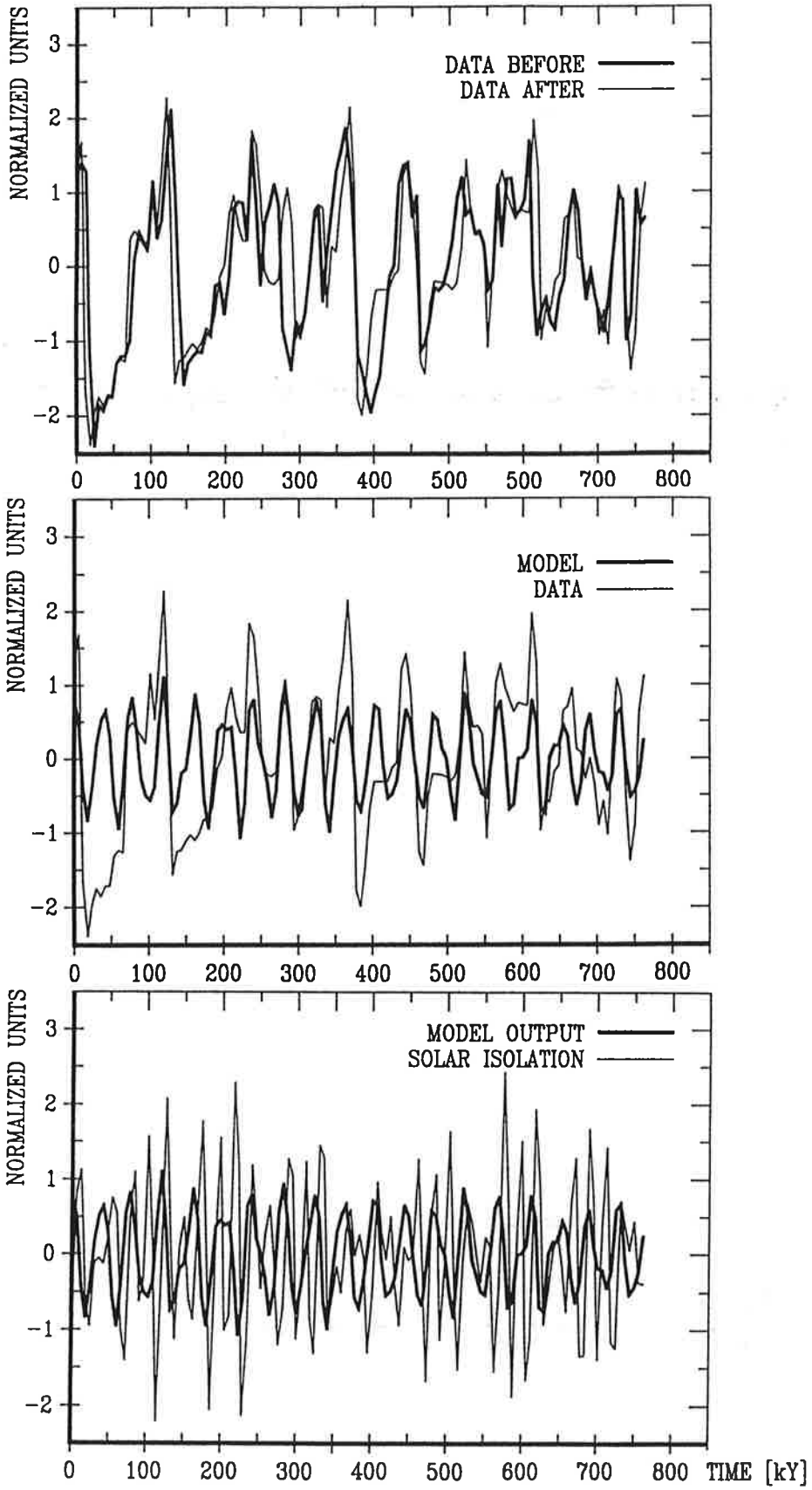

Figure 8: The top panel shows the data curves before and after optimization, while in the middle the data time series is plotted versus model output, which can be seen at the bottom again compared to solar insolation.

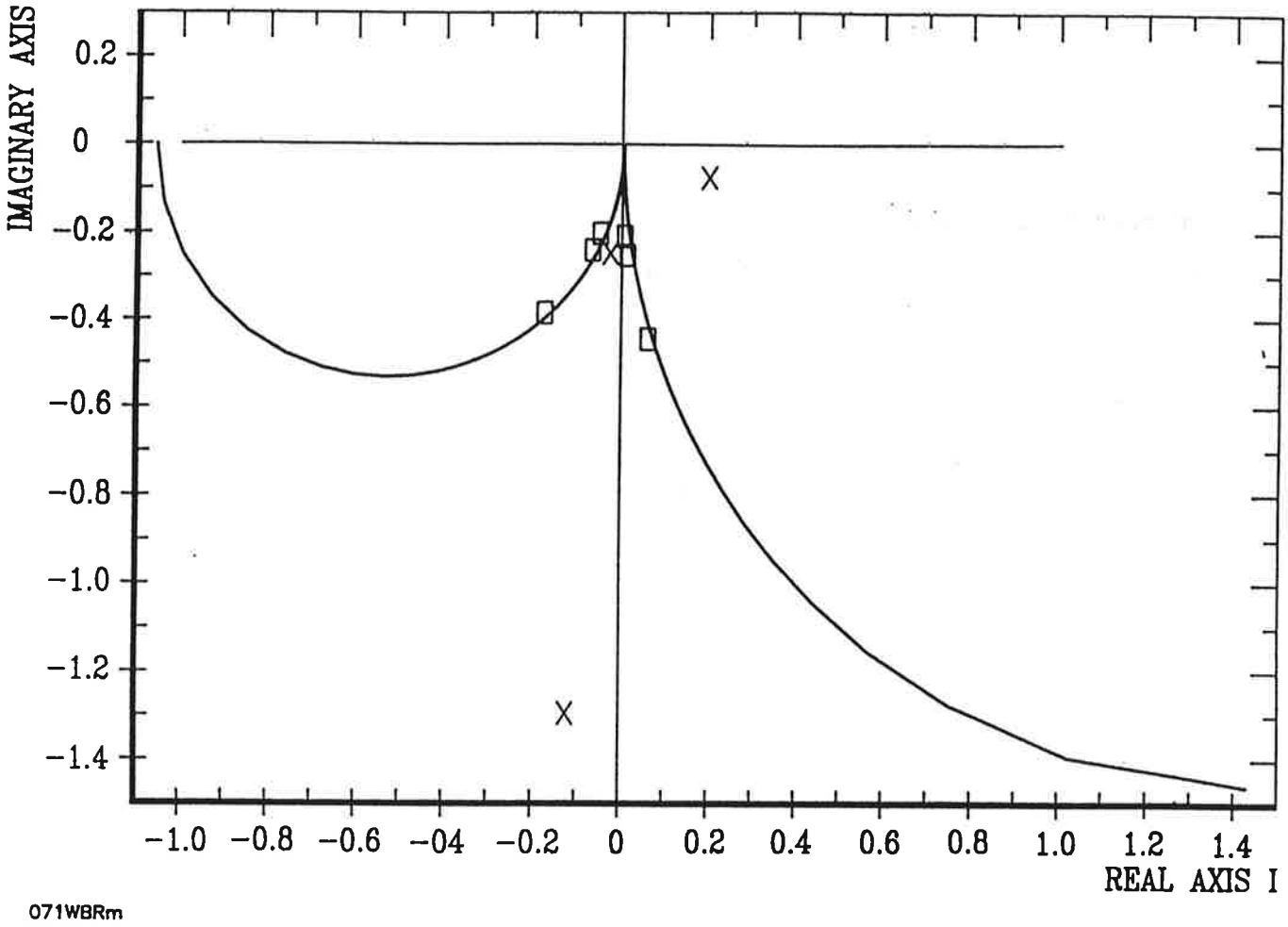

Figure 9: Optimal transfer function (indicated by the crosses for the Milankovitch frequencies) and preferred transfer function (full lines). The full line on the right hand side is the transfer function of the preferred model for $\lambda = 0.024$ and $\alpha = 0.07$. The full line on the left hand side shows the graph of formula (4) for $\lambda = -0.06$. The distance between the optimal and the preferred transfer function does not depend strongly on the sign of λ.

data variance cannot be explained by a linear model with input solar insolation. This result is not surprising considering the large climate response and negligible solar forcing in the 100 ky band. Imbrie and Imbrie [1980] and Martinson et al. [1987] have suggested for this reason the use of a non-linear model consisting of two different linear models for cooling and warming periods, an approach which is motivated by the typical asymmetric shape of the data curves. Since the main data variance cannot be satisfactorily explained by a linear model, the least-squares function (18) leads to a minimization problem with large residuals. The value of the objective function at the optimal solution is approximately 65% of the value at the starting point.

The results obtained by this approach for the age-depth function are consistent with earlier investigations. The ages of isotopic events determined in core Meteor M 13519 [Sarnthein et al., 1984] are compared with those obtained by Herterich and Sarnthein [1984], Herterich [1988], Imbrie et al. [1984] and Shackleton and Matthews [1977] in table 1 (fine temporal resolution for the last ice-age cycle) and table 2 (coarse temporal resolution).

The deviations between the different approaches tend to be larger in the center of the time interval considered, away from the well-dated end points. The highest amplitudes in the correction x (see figure 3) lie in the time interval between 200 ky and 500 ky, in which the greatest deviations between the three different age-depth relations obtained by Herterich and Sarnthein [1984] are found. Grieger [1991] achieves an age-depth function very similar to our optimal result in the standard run, despite the fact that he neglected the low-frequency component in his model. Martinson et al. [1987] arrive at age-depth relations for another core that show departures from linearity which are similar to those obtained here in the standard run.

The amplitudes and phase shifts of the data spectrum against system input are comparable to the values given by Hasselmann and Herterich [1983] for the age-depth relations CARPOR, TUNE and STUNE.

The maximum coherencies obtained (greater than 90%) are higher than those given by Herterich and Sarnthein [1984] (maximum in single peaks of 75% squared coherency which corresponds to approximately 85% coherency), even though

Table 1: Ages of Isotopic Events				
Isotopic Events cf. Prell et al. [1986]	Depth [cm]	Age [ky]		
		Herterich	Imbrie	Brüggemann
0.0	0.0	0.0	0.0	0.0
1.1	14.0	9.0	6.0	5.9
2.0	26.0	16.4	12.0	12.5
2.2	32.0	20.3	19.0	18.0
3.0	36.4	22.9	24.0	22.8
3.1	42.8	27.0	28.0	31.0
3.3	80.0	52.2	53.0	58.1
4.0	90.7	60.2	59.0	63.2
5.0	96.3	64.5	71.0	65.9
5.1	115.0	79.5	80.0	78.0
5.2	128.4	90.4	87.0	95.3
5.3	138.0	98.0	99.0	102.2
5.4	145.3	103.5	107.0	105.6
5.5	168.6	120.0	122.0	119.7
6.0	184.0	129.7	128.0	127.6

Table1: Ages of the isotopic events in core Meteor M 13519 during the last 130 ky. The core data and the third column are taken from Herterich [1988], while the fourth column shows the SPECMAP results given by Imbrie et al. [1984].

Table 2: Ages of Isotopic Events							
Isotopic Event	Depth [cm]	Age [ky]					
		CAR.	TUNE	STUNE	SHACK	SPEC.	Brü.
1/ 2	24.0	13	17	10	13	12	11
2/ 3	38.0	27	31	18	32	24	25
3/ 4	83.0	56	73	49	64	59	60
4/ 5	98.0	70	86	63	75	71	67
5/ 6	184.0	127	139	127	128	128	128
6/ 7	277.0	209	195	184	203	186	203
7/ 8	370.0	277	260	244	262	245	289
8/ 9	416.0	312	290	269	310	303	306
9/10	506.0	374	348	332	362	339	375
10/11	558.0	410	381	369	383	362	395
11/12	622.0	444	420	409	459	423	458
12/13	685.0	510	478	475	492	478	519
13/14	744.0	540	526	527	524	524	549
14/15	758.0	551	537	539	565	565	560
15/16	829.0	608	591	598	617	620	622
16/17	884.0	657	635	644	654	659	649
17/18	916.0	678	658	668	675	689	677
18/19	968.0	712	701	712	712	726	719
19/20	996.0	733	720	730	736	736	739

Table2: Ages of the stage boundaries (defined by Shackleton and Opdyke [1973]) in core Meteor M 13519 for the full length of the core. The depths are taken from Sarnthein et al. [1984]. The three tuning approaches CARPOR (CAR.), TUNE and STUNE are given by Herterich and Sarnthein [1984] which also lists the SHACK data from Shackleton and Matthews [1977]. The SPECMAP (SPEC.) age-depth function is given by Imbrie et al. [1984].

coherency is not explicitly contained in our objective function F in (18). The coherencies are slightly lower than those given by Imbrie et al. [1984] for the SPECMAP time scale, although it should be pointed out that the SPECMAP coherencies are calculated between an artificial stack and the sum of the normalized orbital parameters (ETP). By using the ETP curve as system input, the SPECMAP approach is also able to explain data energy contained in the 100 ky cycle, where there is no significant energy in solar insolation.

Application to different cases

In order to test the method with different combinations of input data series, tuning targets and first guess age–depth functions, we performed the following sensitivity studies:

- SPECMAP stack with the standard first guess age-depth function and tuning target solar insolation (case 1)
- core M 13519 with first guess age-depth function given by a linear interpolation between isotopic stage boundaries dated by the SPECMAP calibration (case 2)
- core M 13519 with a first guess age-depth function given by a linear interpolation between the present and the re-dated Brunhes-Matuyama boundary at 780 ky with Δt increased from 6 ky to 7 ky (case 3)
- SPECMAP stack with a first guess age-depth function given by a linear interpolation between isotopic stage boundaries optimally dated by the standard run (case 4)
- SPECMAP stack with a first guess age-depth function given by a linear interpolation between the present and the re-dated Brunhes-Matuyama boundary at 780 ky with Δt increased from 6 ky to 7 ky (case 5)
- SPECMAP stack with the standard first guess age-depth function but the tuning target ETP (case 6)

The results (spectra of the data before and after optimization, corresponding coherencies and optimized time series compared to the SPECMAP stack) are

shown in figures 10 – 15.

Note that in the case of ETP-forcing (case 6) it is possible to improve the SPECMAP calibration in terms of the coherencies, although this was the SPECMAP optimization criterion. The optimal time constant of the preferred system in this case is 12.8 ky.

The coherencies obtained for the SPECMAP case with a first guess age-depth relation taken from the optimal standard run (case 4) are quite high, although only forcing by solar insolation is considered, but do not reach the values obtained in case 6. This observation and the fact that the optimal solutions for the standard case and case 2 are quite different suggests that the optimization problem has (a probably large number of) local minima. Reasonable coherency values were also obtained for the two cases (case 3 and case 5) that were started with a first guess age-depth function that attributes an age of 780 ky to the Brunhes Matuyama boundary instead of 730 ky. This gives further support to the redating of the Brunhes–Matuyama boundary as suggested by Shackleton et al. [1990].

Random Time Series and Sensitivity Analysis for Weights

It has been shown that high coherencies in all three Milankovitch frequencies can be obtained for real ocean core data by optimizing the age-depth function. There is naturally a lingering suspicion that this may just be an artifact of the analysis method, and that high coherencies could have been generated artificially for any random time series. To rule out this possibility, a filtered white noise test was performed, in which the input time series was generated randomly with a spectrum similar to that of a typical $\delta^{18}O$ data series (i.e., most energy contained in the 100 ky frequency band). Again, corrections of a similar shape were produced and a similar energy shift from the 100 ky to the 41 ky band could be observed, but significant coherencies could be generated in only one frequency band at a time. It was impossible to obtain simultaneously reasonable coherencies in all three Milankovitch bands, as found for real ocean core data.

The weights g_i served two purposes. First, they were used to normalize the different components of the objective function, which is necessary for numerical

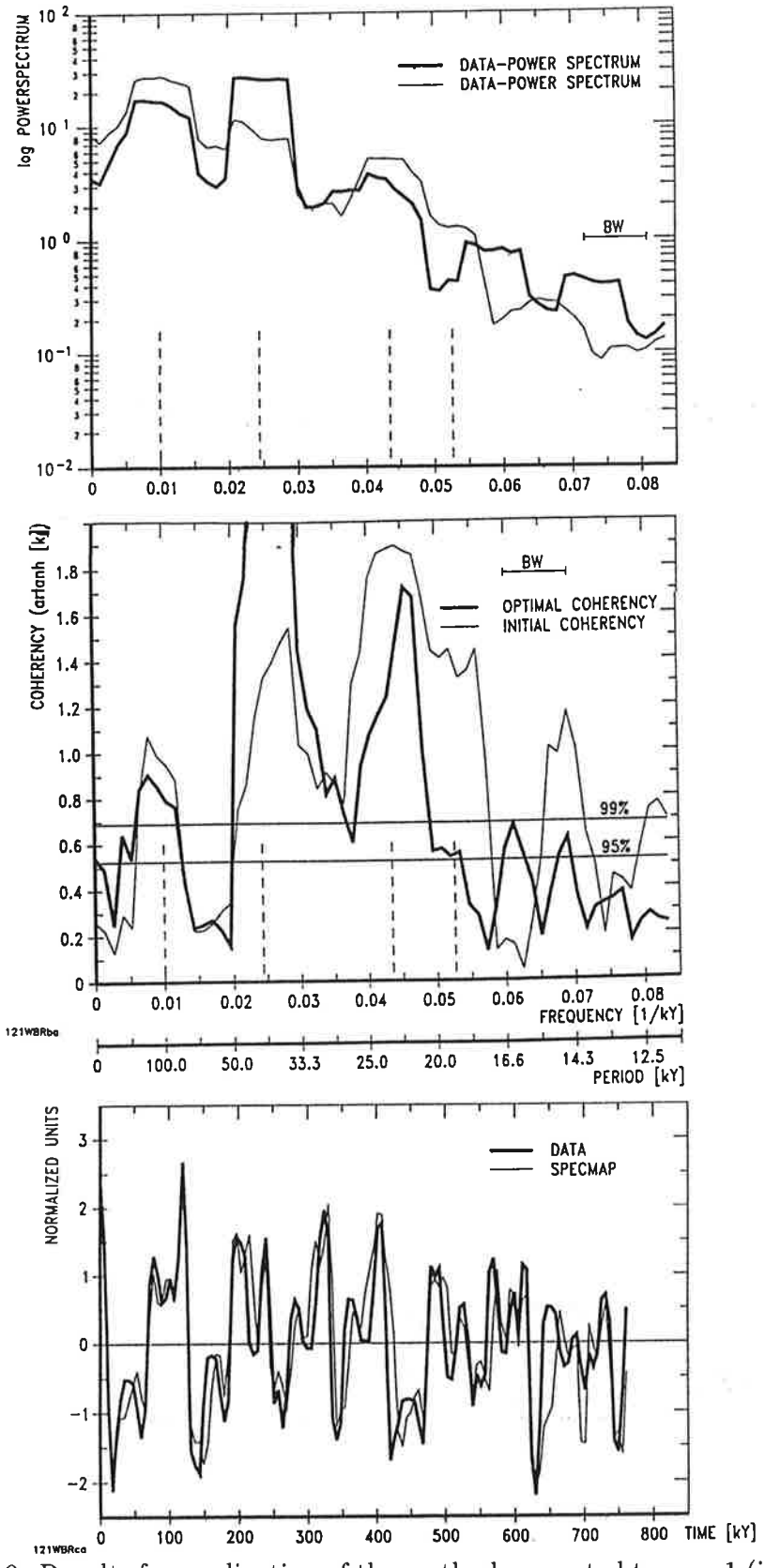

Figure 10: Results for application of the method presented to case 1 (i.e., SPECMAP stack with the standard first guess age-depth function and tuning target solar insolation). The top panel shows the spectra before (thin line) and after optimization (bold line), while the associated coherencies are shown in the middle panel. At the bottom the optimized data curve and the SPECMAP stack are plotted versus time.

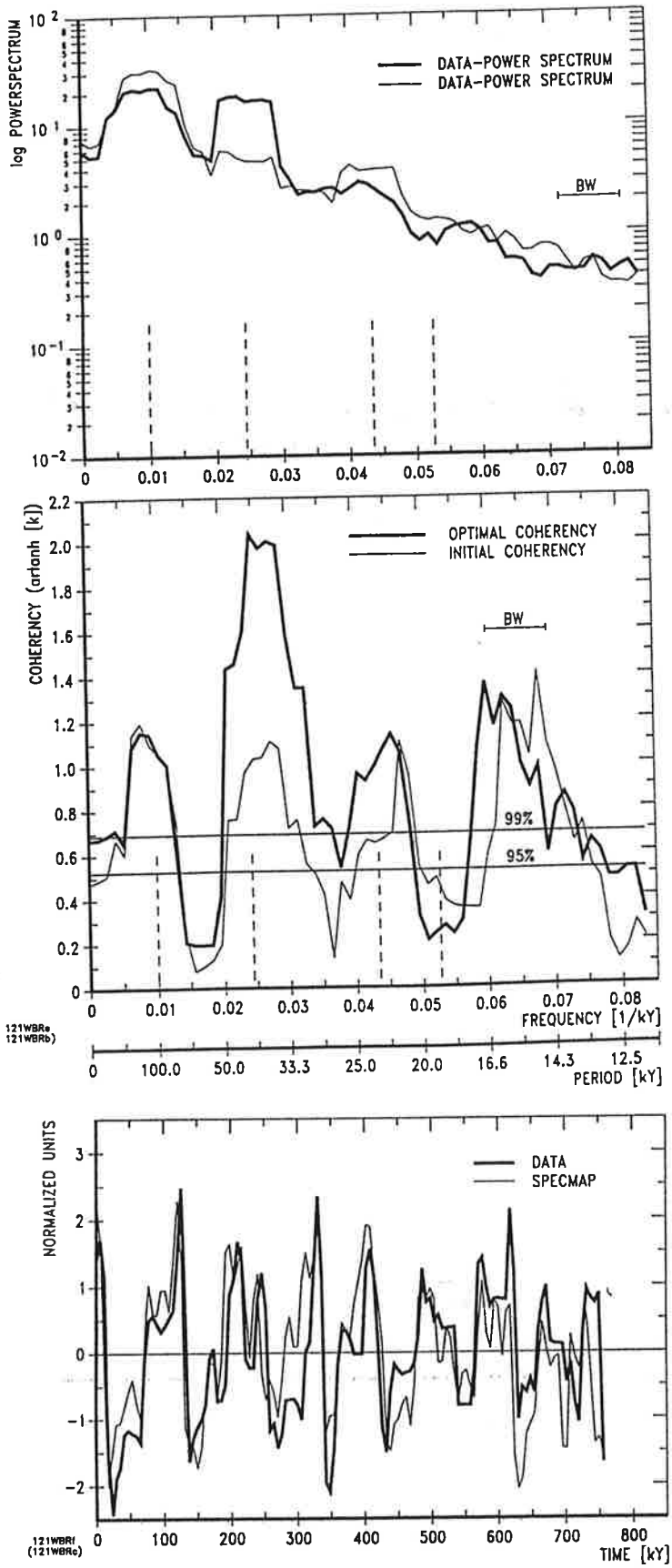

Figure 11: As for figure 10, but for case 2 (i.e., core M 13519 with a first guess age-depth function given by a linear interpolation between isotopic stage boundaries dated by the SPECMAP calibration).

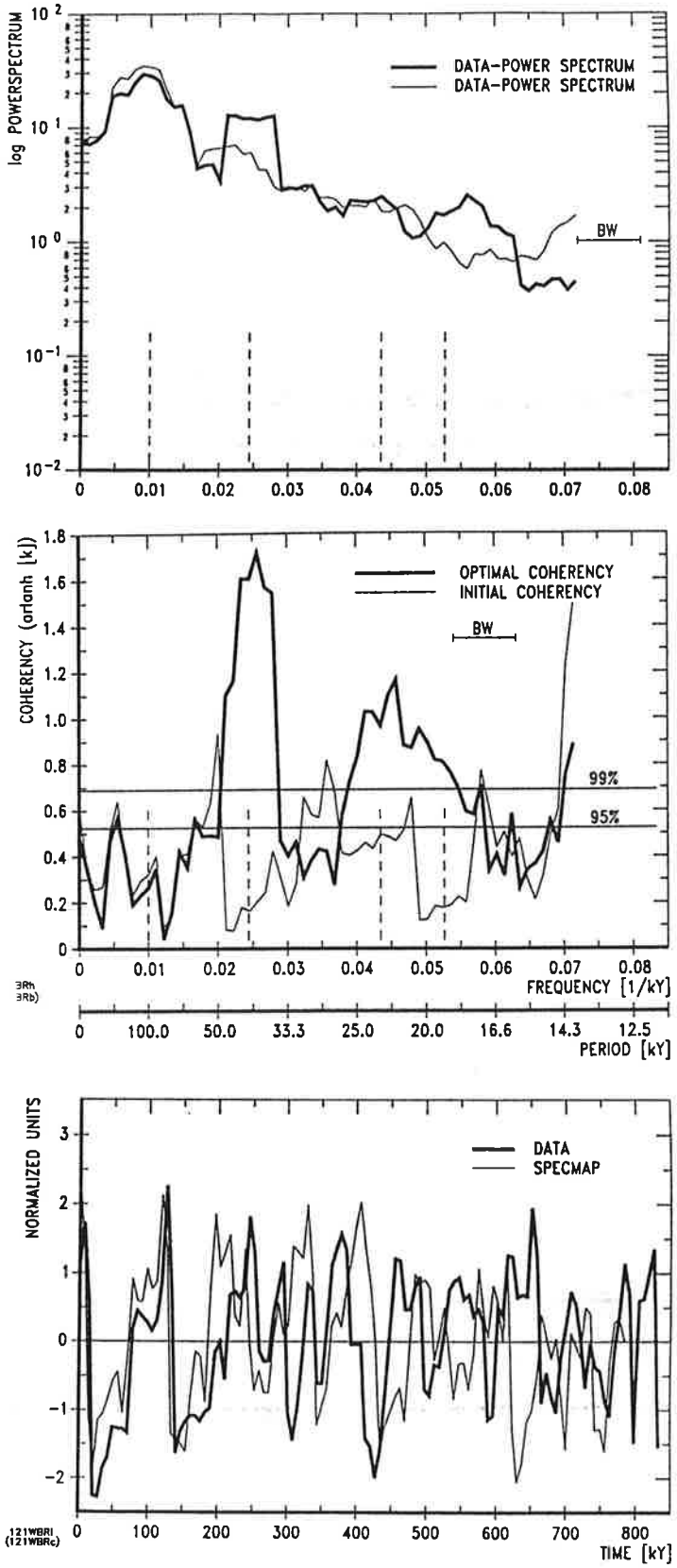

Figure 12: As for figure 10, but for case 3 (i.e., core M 13519 with a first guess age-depth function given by a linear interpolation between the present and the re-dated Brunhes-Matuyama boundary at 780 ky).

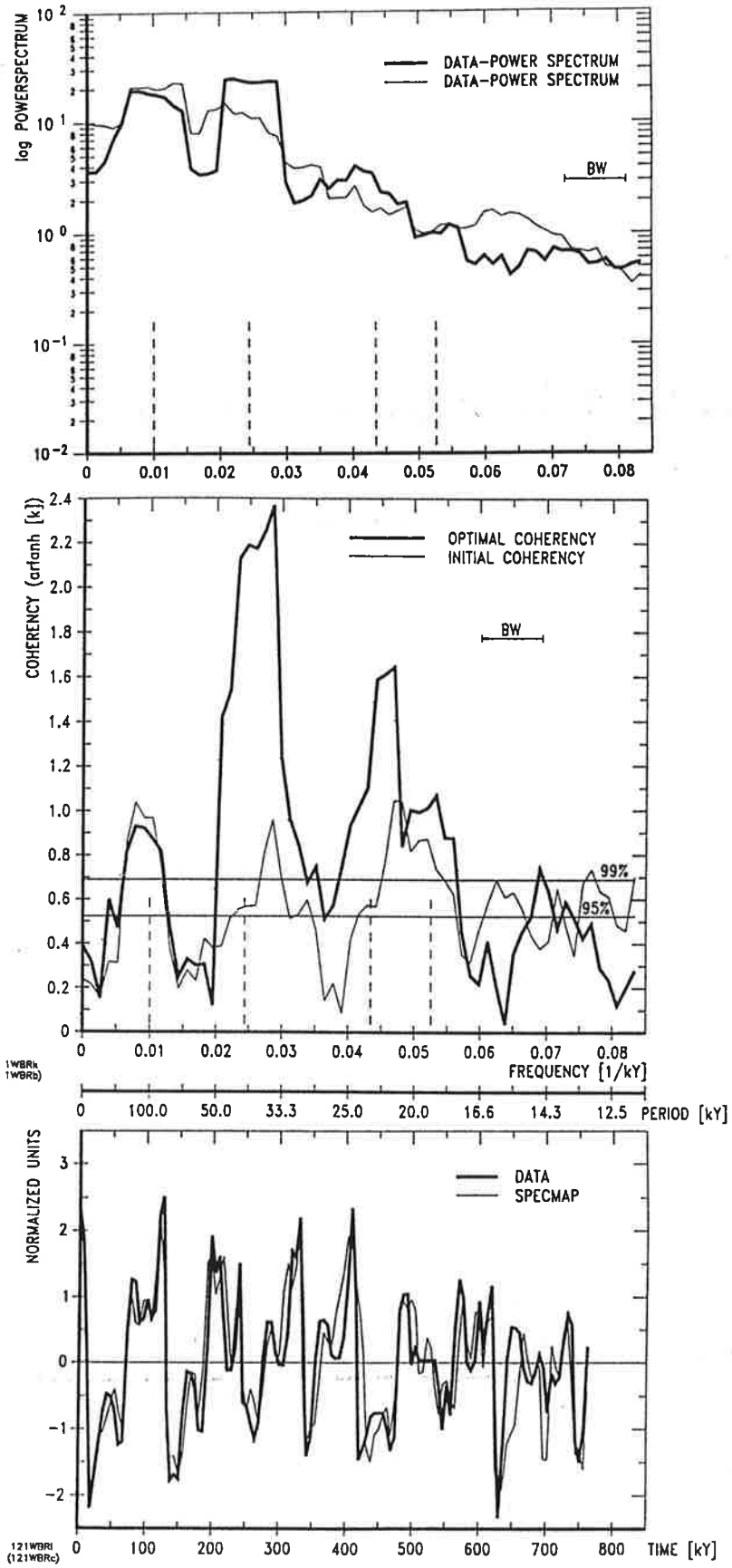

Figure 13: As for figure 10, but for case 4 (i.e., SPECMAP stack with a first guess age-depth function given by a linear interpolation between isotopic stage boundaries optimally dated by the standard run).

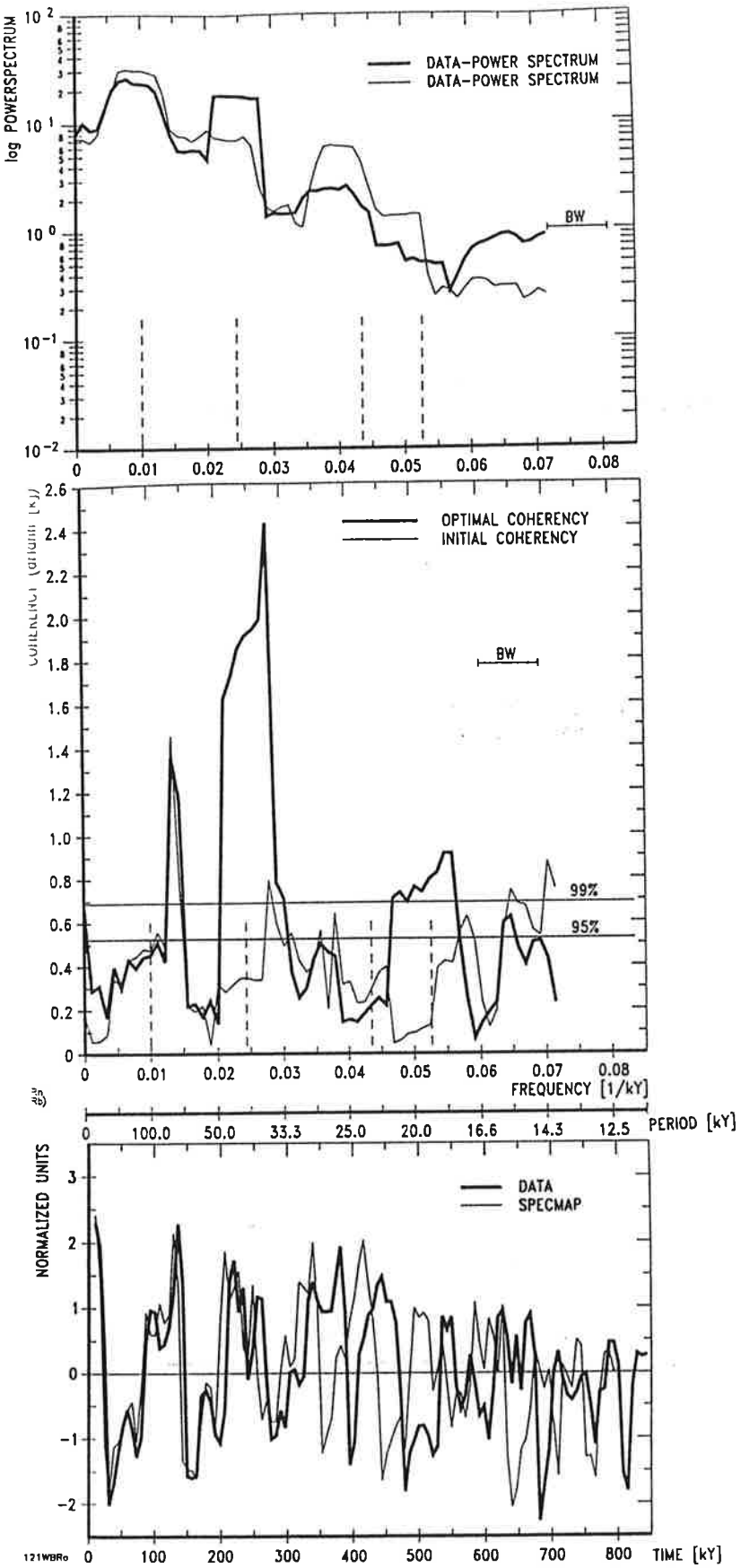

Figure 14: As for figure 10, but for case 5 (i.e., SPECMAP stack with a first guess age-depth function given by a linear interpolation between the present and the re-dated Brunhes-Matuyama boundary at 780 ky).

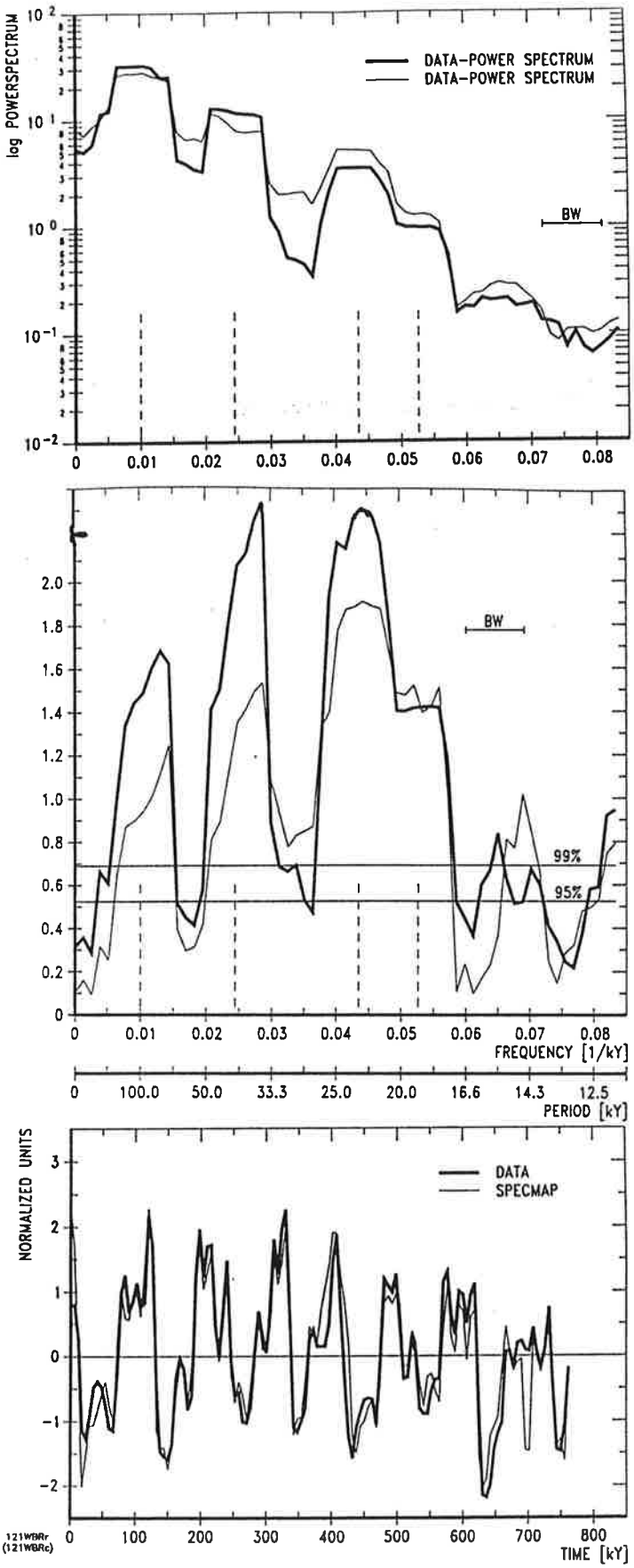

Figure 15: As for figure 10, but for case 6 (i.e., SPECMAP stack with the standard first guess age-depth function but tuning target ETP).

stability. Second, they reflect the subjective judgement of the user as to the respective importance of the different components. For physically meaningful age-depth functions we always selected large values for the weight g_6. Since the corresponding objective function component is zero for a linear age-depth function, this does not contribute to the initial iterations of the objective function and acts only to prevent solutions from becoming non-monotonic. To test the sensitivity of the minimization problem with respect to the remaining weights $g_1, \ldots, g_5$ we computed standard case solutions for weights which were individually multiplied by factors

$$\frac{1}{100}, \frac{1}{10}, 10 \text{ and } 100$$

while all other weights were kept at their standard run values. The highest coherencies were obtained in the standard run. The basic low-frequency structure (cycle length of 250 ky and more) of the optimal age-depth function remains constant throughout the sensitivity analysis, although the high-frequency details (in this context: cycle lengths at 100 ky and less) varied considerably. This preliminary sensitivity analysis yields age-depth functions with differently shaped corrections. As expected, a much smoother correction was obtained, when the parameter for the second derivative was increased.

Another question is the influence of the first guess age-depth function and the starting values of the parameters α and λ. Since the objective function is neither quadratic nor convex, we may expect several local minima. In general, there is no guarantee that numerical optimization routines will locate the global minimum, although there are algorithms that cope with this problem (e.g. the Simulated Annealing approach developed by Kirkpatrick et al. [1983] originating from equation of state calculations in thermodynamics by Metropolis et al. [1953]). Additional minima can be obtained by changing the first guess, as indicated in the above discussed case studies. We performed a further numerical test where the first guess age-depth relation was altered from a linear function by adding randomly-selected corrections drawn from the interval $[-3\text{cm}, 3\text{cm}]$. The result from this experiment did not differ significantly from the standard run. In general, the optimization problem is more sensitive to the weights than to small changes of the first guess age-depth function, although substantial changes of this function will alter the results considerably (e.g., SPECMAP calibration ver-

sus linear interpolation). Thus, if a priori information about the data indicate that a linear age-depth function is incorrect, this information should be used to determine a better reference first guess age–depth function. For example, if the linear age-depth function incorrectly maps a peak of the data curve to an input peak, the algorithm is not likely to change this incorrect matching, since this would usually imply a temporary increase of the objective function, which is usually not allowed in deterministic optimization algorithms.

6 Summary and Conclusions

The mathematical approach suggested by Hasselmann and Herterich [1983] represented an attempt to optimize simultaneously the age-depth function and a linear response model. In this investigation, we have implemented and improved this approach, using a completely different numerical solution strategy. The method presented here provides a universal tool for core calibration and testing of linear relationships between different forcing mechanisms and the response of the climate system on ice-age time scales. It was possible to improve the SPECMAP calibration in terms of the obtained coherencies. The optimal results for the age-depth function of an ocean sediment core are comparable to those given by Herterich and Sarnthein [1984], Imbrie et al. [1984] and Shackleton and Matthews [1977] with energy contained in the spectrum of the correction function itself in a broad band around 100 ky. The coherencies are higher than in Herterich and Sarnthein [1984] and comparable to those obtained by Imbrie et al. [1984]. It was possible to transfer energy in the data spectrum from the 100 ky band to the Milankovitch frequency bands, especially at 41 ky, where significant energy was not contained previously.

However, a large fraction of the energy contained in the data spectrum, particularly in the 100 ky frequency band, cannot be explained by a linear model using solar insolation as input. The saw-tooth shape of the data curve suggests that a non-linear model, such as that proposed by Imbrie and Imbrie [1980], may be required. The tuning of age-depth functions to a non-linear model is more complicated than the case considered here, but is in principle amenable to the

same techniques.

The main goal of this investigation, however, was to develop an automatic time calibration and dynamical model fitting technique which can be applied to many cores. In order to develop a global picture of the structure of the late Pleistocene climate cycles, it will be necessary to optimize simultaneously the age-depth functions for a number of different cores within the context of a global dynamical model, a task which can be addressed only with the aid of a general inversion method.

7 Acknowledgements

This work was developed from a Diplomarbeit (Master's Thesis) at the Institut für Angewandte Mathematik der Universität Hamburg and the Max-Planck-Institut für Meteorologie in Hamburg. In writing my thesis and this article I have received help and advice from many people. In particular, I would like to thank G. Opfer and K. Hasselmann for their support and advice and K. Herterich, B.D. Santer and T.J. Crowley for helpful discussions. All computations were carried out on the Cray-2 of the Deutsches Klimarechenzentrum (DKRZ) in Hamburg. M. Sarnthein provided the data series for the core M 13519, while W. Howard supplied the SPECMAP and ETP data from J. Imbrie et al.. A. Berger provided a computer program to calculate solar insolation in the past. During visits with L. Labeyrie at the Centre des Faibles Radioactivités (CRNS) in Gif sur Yvette, France, and with M. Sarnthein at the Geologisches-Paläontologisches Institut (CAU) in Kiel I learnt the basics about the extraction of the data from deep-sea cores. The figures were drawn expertly by M. Grunert.

References

Berger, A.L., A Simple Algorithm to Compute Long Term Variations of Daily or Monthly Insolation, Institut d'Astronomique de Louvian, Contribution No. 18, 1978.

Brüggemann, W., Optimierung der Alterstiefenzuordnung von Tiefseebohrkernen, Universität Hamburg, Diplomarbeit 1990.

Crowley, T.J., and G.R. North, Paleoclimatology, Oxford University Press, New York, and Clarendon Press, Oxford, 1991.

Gill, P.E., and W. Murray, Conjugate-Gradient Methods for Large-Scale Nonlinear Optimization, Technical Report SOL 79 – 15, Systems Optimization Laboratory, Department of Operations Research, Stanford University, Stanford CA, 1979.

Gill, P.E., W. Murray and M.H. Wright, Practical Optimization, Academic Press, London, 1981.

Grieger, B., Orbital tuning of marine sedimentary cores, An automatic procedure based on a general linear model, unpublished working paper, Max-Planck-Institut für Meteorologie, Hamburg, June 17th 1991.

Hasselmann, K. and K. Herterich, Application of Inverse Modelling Techniques to Palaeoclimatic Data, in *Paleoclimatic Research and Models* edited by A. Ghazi, pp. 52 - 68, D. Reidel Publishing Company, Dordrecht, 1983.

Hays, J.D., J. Imbrie and N.J. Shackleton, Variations in the Earth's Orbit: Pacemaker of the Ice Ages, *Science, 194*, 1121 - 1132, 1976.

Herterich, K., and M. Sarnthein, Brunhes Time Scale: Tuning by Rates of Calcium-Carbonate Dissolution and Cross Spectral Analyses with Solar Insolation, in *Milankovitch and Climate, Part 1* edited by A.L. Berger, J. Imbrie, J.D. Hays, G. Kukla and B. Saltzman, pp. 447 - 466, D. Reidel Publishing Company, Dordrecht, 1984.

Herterich, K., Extracting the Parameters of Simple Climate Models by Inverse Modeling of the Deep–Sea Core Climatic Record, Report No. 23 des Max–Planck–Institutes für Meteorologie, Hamburg, 1988.

Hilgen, F.J., Astronomical calibration of Gauss to Matuyama sapropels in the Mediterranean and implication for the Geomagnetic Polarity Time Scale, *Earth and Planetary Science Letters, 104*, 226 - 244, 1991.

Imbrie, J. and J.Z. Imbrie, Modeling the Climatic Response to Orbital Variations, *Science, 207*, 943 - 953, 1980.

Imbrie, J., J.D. Hays, D.G. Martinson, A. McIntyre, A.C. Mix, J.J. Morley, N.G. Pisias, W.L. Prell and N.J. Shackleton, The Orbital Theory of Pleistocene Climate: Support from a Revised Chronology of the Marine $\delta^{18}O$ Record, in *Milankovitch and Climate, Part 1* edited by A.L. Berger, J.Imbrie, J.D. Hays, G. Kukla and B. Saltzman, pp. 269 - 305, D. Reidel Publishing Company, Dordrecht, 1984.

Izett, G.A., and J.D. Obradovich, Dating of the Matuyama–Brunhes Boundary Based on $^{40}Ar/^{39}Ar$ Ages of the Bishop Tuff and Cerro San Luis Rhyolite, Abstract, Geological Society of America, San Diego, October 21–24, 1991.

Jenkins, G.M., and D.G. Watts, Spectral Analysis and its Applications, Holden-Day, Oakland, 1968.

Kirkpatrick, S., C.D. Gelatt, Jr., and M.P. Vecchi, Optimization by Simulated Annealing, *Science, 220,* pp. 671 - 680, 1989.

Martinson, D.G., N.G. Pisias, J.D. Hays, J. Imbrie, T.C. Moore and N.J. Shackleton, Age Dating and the Orbital Theory of the Ice Ages: Development of a High–Resolution 0 to 300 000-Year Chronostratigraphy, *Quarternary Research, 27*, 1 - 29, 1987.

Metropolis, N., A.W. Rosenbluth, M.N. Rosenbluth, A.H. Teller and E. Teller, Equation of State Calculations by Fast Computing Machines, *J. Chem. Phys., 21*, 1087 - 1092, 1953.

Milankovitch, M., Astronomische Mittel zur Erforschung der erdgeschichtlichen Klimate, *Handbuch der Geophysik IX, Band 3*, edited by B. Gutenberg, pp. 593 - 698, Verlag Gebrüder Borntraeger, Berlin, 1938.

Prell, W.L., J. Imbrie, D.G. Martinson, J.J. Morley, N.G. Pisias, N.J. Shackleton and H.F. Streeter, Graphic Correlation of Oxygen Isotope Stratigraphy Application to the Late Quaternary, *Paleoceanography, 1*, 137 - 162, 1986.

Sarnthein, M., H. Erlenkeuser, R. von Grafenstein and C. Schröder, Stable-isotope Stratigraphy for the last 750 000 Years: "Meteor" Core 13519 from the eastern equatorial Atlantic, *"Meteor" Forschungsergebnisse, Berlin, Stuttgart, Reihe C, No. 38*, 9-24, 1984.

Shackleton, N.J., A. Berger and W.R. Peltier, An alternative astronomical calibration of the lower Pleistocene timescale based on ODP Site 677, *Transactions of the Royal Society of Edinburgh: Earth Sciences, 81*, 251 - 261, 1990.

Shackleton, N.J., and R.K. Matthews, Oxygen Isotope Stratigraphy of Late Pleistocene Coral Terraces in Barbados, *Nature, 268*, 618 - 620, 1977.

Shackleton, N.J., and N.D. Opdyke, Oxygen Isotope and Paleomagnetic Stratigraphy of Equatorial Pacific Core V28-238: Oxygen Isotope Temperatures and Ice Volumes on a 10^5 Year and 10^6 Year Scale, *Quarternary Research, 3*, 39 - 55, 1973.

Walter, R.C., P.C. Manega, R.C. Hay, R.E. Drake, and G.H. Curtis, Laser-fusion $^{40}Ar/^{39}Ar$ dating of Bed I, Olduvai Gorge Tanzania, *Nature, 354*, 145 - 149, 1991.